Water properties inside nanoscopic hydrophobic pocket studied by computer simulations

Piotr Setny[a] and Maciej Geller
Biophysics Department, Warsaw University, Zwirki i Wigury 93, 02-089 Warsaw, Poland

(Received 12 May 2006; accepted 23 August 2006; published online 13 October 2006)

The structure and dynamics of water in the vicinity of the hemispherical hydrophobic pocket of 8 Å radius were examined via molecular dynamics simulations in *NVT* ensemble. Density, hydrogen bonding properties, and residence times of water molecules were projected on two-dimensional planes providing a spatial description of water behavior. We found that the average water density is significantly depleted relative to bulk value. A detailed analysis of pocket occupancy revealed fluctuations between states of completely empty pocket and a pocket filled with a bulklike fluid, which seem to result from collective behavior of water molecules. Free energy differences accompanying these fluctuations are rather small, suggesting that the given pocket radius is close to the critical one for transition between gas and liquid phases in the considered system. We show that the situation is different in the case of a simple Lennard-Jones fluid. These results indicate that changing the surface curvature from flat to concave may lead to qualitative difference in water behavior in its vicinity. We think that our studies may also put some light on binding site desolvation process which is necessary to understand to make correct predictions of binding energies. © *2006 American Institute of Physics*. [DOI: 10.1063/1.2355487]

I. INTRODUCTION

Hydrophobic interactions manifest themselves as a tendency of relatively apolar molecules to stick together in aqueous solution.[1,2] They play a key role in the formation of large biological structures,[3] protein folding,[4] and ligand binding.[5] Their origin comes from rearrangement of water shell surrounding solvated molecules[6] and desolvation of interacting surfaces, but the exact mechanism is still under debate.[7]

Structure and properties of water around small species are relatively well investigated.[8–12] A picture has emerged according to which water molecules form a solvation shell[13,14] of higher density than surrounding bulk, being able to effectively reorganize, and maintain maximum number of hydrogen bonds with their neighbors. It allows for compensation of enthalpic losses related to the insertion of hydrophobic object but is also accompanied by significant decrease in entropy, which leads to overall positive free energy of solvation.

Situation changes when it comes to large objects. Neighboring water molecules are geometrically unable to maintain maximum number of hydrogen bonds and are forced to point one of their hydrogens towards the nonpolar surface.[15–17] This leads to enthalpic penalty, resulting in a threefold greater surface tension for planar surfaces when compared to small molecules.[1]

Furthermore, according to theoretical works by Chandler and co-workers,[18–22] the interface between water and large hydrophobic objects is more likely to resemble liquid-vapor boundary than the first solvation shell present around small objects. Scaled particle theory[23,24] also predicts a depletion of density of water molecules in contact with hydrophobic cavities of radii greater than 10 Å.

Such predictions seem to be confirmed by various experimental studies mostly based on neutron reflectivity[25,26] and x-ray reflectivity.[27] They report a region of reduced water density at a hydrophobic surfaces ranging from 1 to 4 nm. There is also some evidence of gas-filled submicrocavities, existing close to the surface,[28–31] whose nucleation, as two surfaces approach each other, may be a possible explanation of origin of long-range attractive forces observed in atomic force microscopy.[32] Other studies,[33,34] however, do not support the idea of preexisting nanobubbles. In general, it should be noted that quantitative results of such measurements depend on the type and concentration of dissolved gases as well as on molecular structure of a given hydrophobic surface.[25]

Early explicit solvent simulations of water near large, flat surfaces[16,17] did not reveal its tendency to form a vaporlike interface. More recent works, however, concerning properties of water between two nanoscale hydrophobic ellipsoidal plates[35] or two hydrophobic surfaces,[36] report a drying transition to occur in region enclosed between considered objects as the separation between them becomes smaller. In both cases a strong dependence of critical distance for dewetting on the strength of the attractive part of solute-water potential has been indicated. Such dependence has been also demonstrated in simulations of two parallel planar nanoscopic solutes, each constructed as a single layer of carbon atoms aligned in a hexagonal lattice, where drying has been observed only when attractive carbon-water interactions were absent.[37,38]

For large biomolecules whose surfaces have rather com-

[a]Electronic mail: piosto@icm.edu.pl

 © 2006 American Institute of Physics

Downloaded 08 Nov 2006 to 144.74.27.1. Redistribution subject to AIP license or copyright, see http://jcp.aip.org/jcp/copyright.jsp

plex topography also a shape dependence of hydrophobic effects is of great importance.[39] A dewetting, if present, would preferably occur in concave regions. In their experimental and simulation study Barrat *et al.*[40] analyzed a ligand binding to the mouse major urinary protein. They have concluded that possible dewetting of hydrophobic pocket prior to ligand binding is a key factor influencing the thermodynamic signature of binding. In simulations of water droplet enclosed in a large spherical hydrophobic cavity, Wallqvist *et al.*[41] have not found a stable vaporlike interface when attractive water-surface interactions were taken into account. Instead they have observed an intermediate state between "dry" and "wet," referred to as a "contact" state, which was characterized by abrupt decrease in water density from bulklike to zero without preceding density oscillations. These results confirm observations obtained earlier in simulations of water inside hydrophobic spherical cavities that were considered as a reference system for reverse micelles.[42] On the other hand, Chau[43] who investigated water behavior around hemispherical objects of various radii reports a clearly layered structure of water molecules in the concave region. Although he has found depletion of average density of water inside hemispheres as their radius has been decreased, no evident drying has been detected.

Studies of hydrophobic cylindrical pores bring differing results as well. Beckstein and Sansom[44] investigated liquid-vapor oscillations of water in hydrophobic nanopores by molecular dynamics (MD) simulations and observed drying when the pore radius was smaller than 5.5 Å. On the other hand, Hummer *et al.*[45] demonstrated in their MD simulation of carbon nanotube that it can be effectively solvated, even though it is able to accommodate only one-dimensional chain of water molecules. Authors have also noted that a small decrease in magnitude of water-carbon attractive potential leads to qualitative change in water occupancy, which starts to fluctuate between empty and filled states.

It is evident that a better understanding of the hydrophobic hydration of large objects is important. In this article we describe results of simulations of water molecules enclosed by two parallel flat walls containing spherical pockets. We analyze structural properties of water such as density, number of hydrogen bonds, average dipole moments, as well as its dynamics expressed as residence times in various locations. Having regions of flat, convex, and concave interfaces we can directly observe differences between them. We also analyze fluctuations of density of water inside pockets and compare them to bulk density fluctuation.

In order to determine contributions of hydrogen bonding and complex electrostatic interactions between water molecules, we perform parallel simulations of a Lennard-Jones fluid in identical conditions.

II. METHODS

A. The system

Simulated system consisted of two hydrophobic walls and 1030 solvent molecules (Fig. 1). Both walls, having lateral dimensions of 35×33 Å^2, were constructed of neutral particles aligned in a hexagonal close packed (hcp) grid. We

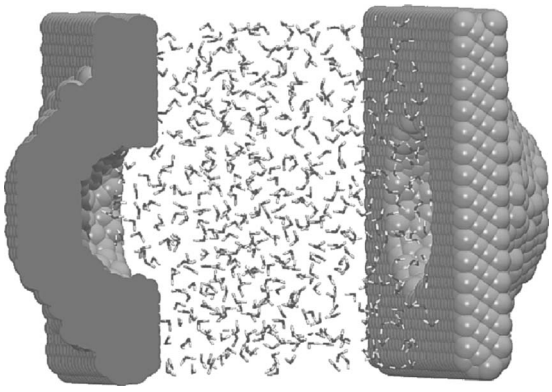

FIG. 1. Simulated system: two hydrophobic walls and 1030 TIP4P water molecules.

assumed that they would represent a paraffin of 0.8 g/cm^3 density, composed of CH_2 units. This assumption would lead to a grid of 3.5 Å lattice constant. In such case four layers of CH_2 pseudoatoms would produce the wall of 7.5 Å thickness.

However, to be able to construct more detailed pockets, we decided to use a finer grid, with lattice constant of 1.25 Å. Parameters of Lennard-Jones potential for atoms constituting the simulated wall were fitted to reproduce the potential of original four layers of CH_2 pseudoatoms (Fig. 2). Resulting Lennard-Jones parameters are presented in Table I.

Pockets were constructed by deleting all pseudoatoms located within a given radius from a central atom at the wall surface. Additional pseudoatoms were added at the back side to maintain thickness of the wall not smaller than four atomic layers. For presented simulations we used a hemispherical pocket of 8 Å inner radius. It had a volume of 389 Å^3 (measured from base, located at the surface of the first layer of wall molecules, to border, where water-wall interaction energy was greater than 0.6 kT). Such volume can accommodate on average about 13 molecules of water at standard density.

Both walls were placed symmetrically along the Z axis, making two opposite sides of rectangular box filled with water. The number of water molecules and separation between walls were tuned to obtain a mean water density of

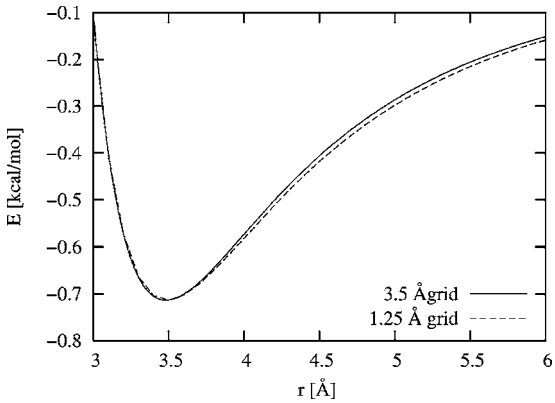

FIG. 2. Water–flat wall interaction potential for four layers of CH_2 pseudoatoms aligned at 3.5 Å hcp grid (solid line) and four layers of modified particles aligned at 1.25 Å grid (dashed line).

Downloaded 08 Nov 2006 to 144.74.27.1. Redistribution subject to AIP license or copyright, see http://jcp.aip.org/jcp/copyright.jsp

TABLE I. Force field parameters. CH_2 (o): original united atom parameters for 3.5 Å grid and CH_2 (m): modified parameters for 1.25 Å grid used in simulation. LJ potential form is $U(r)=4\epsilon[(\sigma/r)^{12}-(\sigma/r)^6]$.

Atom type	ϵ (kcal/mol)	σ (Å)	q (e.u.)
CH_2 (o)	0.1142	3.891	0.0
CH_2 (m)	0.0094	4.100	0.0
	TIP4		
HT	0.0	0.0	0.52
OT	0.1550	3.1535	0.0
OM	0.0	0.0	−1.04
	LJ fluid		
LJ	0.541	2.67	0.0

0.997 g/cm^3 in a $8\times8\times8$ Å^3 at the center of the box. It was achieved by performing three preliminary, 1 ns simulations, each followed by adjustment of system dimensions. As a result the innermost atomic layers of walls were located at $z=\pm15.3$ Å.

Most simulations were performed with TIP4P (Ref. 46) water molecules. Apart from that, however, we have conducted additional simulations with Lennard-Jones fluid in order to determine contributions to system behavior resulting from the complex nature of electrostatic interactions and hydrogen bonds between water molecules. Force field parameters of this fluid (Table I) were the same as used in other studies,[47] in an attempt to best reproduce the pressure of water at a temperature of 300 K and standard number density. Mass of the Lennard-Jones (LJ) particle was also set to equal the mass of water molecule.

Parameters for water-wall interaction were calculated by using the standard Lorenz-Berthelot mixing rules[48] and the same resulting parameters were applied for LJ fluid-wall interaction.

B. Simulations

Although we are aware that the most appropriate ensemble for studying hydrophobic hydration would be *NPT* ensemble, after many considerations we decided to perform our simulations in *NVT* ensemble. We think that using a constant pressure algorithm[49,50] which is best suited for isotropic, solvated systems could introduce some hard to estimate effects in the case of such inhomogeneous system like ours. Secondly, usage of constraints necessary to keep walls in place would add an "external force" to the system which could interfere with proper calculation of internal virial. We think that tuning water density in the center of simulation box (see above) provides a mean pressure reasonably close to the desired 1 atm. We estimate that both pockets together constitute 2.5% of system total volume. Their complete, concominant dewetting would cause pressure fluctuations to be in the order of ±500 bars (for water we assume isothermal compressibility $\kappa_T\approx45\times10^{-6}$ bar^{-1}), which remains in the range of pressure fluctuations observed in *NPT* simulations under atmospheric pressure.

The CHARMM computer program[51] was used to perform molecular dynamics simulations. All simulations were carried out at a temperature of 298 K maintained by the Nose-Hoover thermostat.[52,53] The time step used was 2 fs. The SHAKE (Ref. 54) algorithm was applied to keep TIP4P water molecules rigid. Positions of all pseudoatoms constituting the walls were fixed for all the time of simulation.

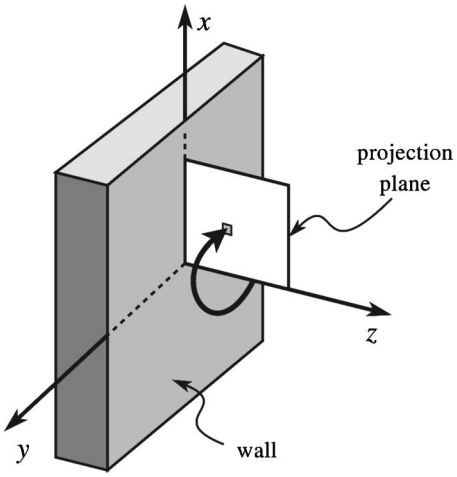

FIG. 3. Projection of structural properties at a two-dimensional plane. An average over toroidal volume is assigned to appropriate intersection on the *XZ* plane.

The particle mesh Ewald summation[55] method was used for electrostatic interactions. Van der Waals interactions were smoothly shifted to zero at a cutoff of 12 Å with the VSHIFT method implemented in CHARMM. Periodic boundary conditions were applied, with box size of 35×33 Å^2 in the *X* and *Y* directions and 100 Å in the *Z* direction in order to eliminate periodic interactions along the *Z* axis.

Each simulation started with 52 ps heating and equilibration phase and then a production run of 1 ns took place. Snapshots of the system were recorded every 0.2 ps.

C. Analysis methods

Analysis of simulation data was performed with a custom program written in C programming language. Cylindrical symmetry of the system along the *Z* axis was used to project all structural parameters on a two-dimensional plane (Fig. 3). They were averaged over toroidal, concentric volumes of 1×1 Å^2 intersection.

We assumed that as long as the average structural data are considered regions close to each wall can be treated as independent. Thus, symmetry of the system with respect to the *XY* plane situated in the middle of the simulation box (at $z=0$) allowed to further average results obtained for each side. The subjects of such analysis were the following.

- Water density, defined as the number of oxygen atoms per unit volume.
- Average hydrogen bond number and each hydrogen bond number (i.e., 0, 1, 2, 3, and 4) fractions. Hydrogen bond was considered as formed based on mixed geometric and energetic criteria:[56] O··H distance lower than 2.4 Å and water-water interaction energy lower than −2.39 kcal/mol (−10 kJ/mol).
- Average hydrogen bond energy.

Downloaded 08 Nov 2006 to 144.74.27.1. Redistribution subject to AIP license or copyright, see http://jcp.aip.org/jcp/copyright.jsp

- Average projection of water dipole moment on the *XZ* plane.

In an attempt to characterize dynamic behavior of the system, we investigated solvent density fluctuations inside both pockets and in the bulk. As the pocket region we considered all points located within the pocket and having $|z|>15.3$ Å. As the bulk region we considered a cylindrical volume of radius of 3.94 Å and height of 8.0 Å placed along the *Z* axis in the center of simulation box. Dimensions of this region were chosen in order to obtain identical volume as in case of both pockets.

Having recorded time distributions of number of solvent molecules inside each area, we calculated free energy profiles related to varying occupancies. We used the following formula:[44]

$$F_n = -k_B T \ln p_n + C,$$

where p_n is a probability of finding n molecules inside the volume and C is an unknown constant.

In order to investigate the shape dependence of dynamic properties, we calculated residence times of solvent molecules in various locations. We considered a number of sites characterized by distance r from the Z axis and by the z coordinate.

Each site was considered "occupied" if a water molecule was found in a spherical volume with radius of 1.5 Å centered on the coordinates of the site. We applied the survival function $S(t)$ (Ref. 57) given by

$$S(t) = \frac{1}{N_{\text{water}}} \sum_{i=1}^{N_{\text{water}}} P_i(t).$$

It gives the fraction of initial number of water molecules N_{water} that remains in a site after a given time t. $P_i(t)$ is a binary function that equals 1 if water i is still in the site after time t, and zero otherwise. Final results for each coordinate pair (r,z) were obtained after averaging $S(t)$ over 16 sites uniformly distributed over a circle of radius r and center at $(0,z)$.

A residence time is often found by a single or double[58] exponential fit to $S(t)$. We have noticed, however, that this procedure gives poor results, especially when applied to water inside the pocket. Thus we decided to use the Kohlrausch-Williams-Watts (KWW) stretched exponential function. It was proved to be useful[59,60] in describing nonexponential relaxations, resulting from superposition of a whole spectrum of single exponential processes, each having its unique relaxation time.[61] It is defined as

$$\phi(t) = e^{-(t/\tau)^{\beta}},$$

where β is called a stretching parameter, which describes the width of the relaxation time constant distribution $(0<\beta \leqslant 1)$. Case of $\beta=1$ corresponds to a single exponential relaxation, when the distribution function is reduced to $\delta(\tau-\bar{\tau})$.

Having estimated values of the τ and β parameters, by fitting KWW curve to $S(t)$, we computed the average relaxation time using the following equation:[61]

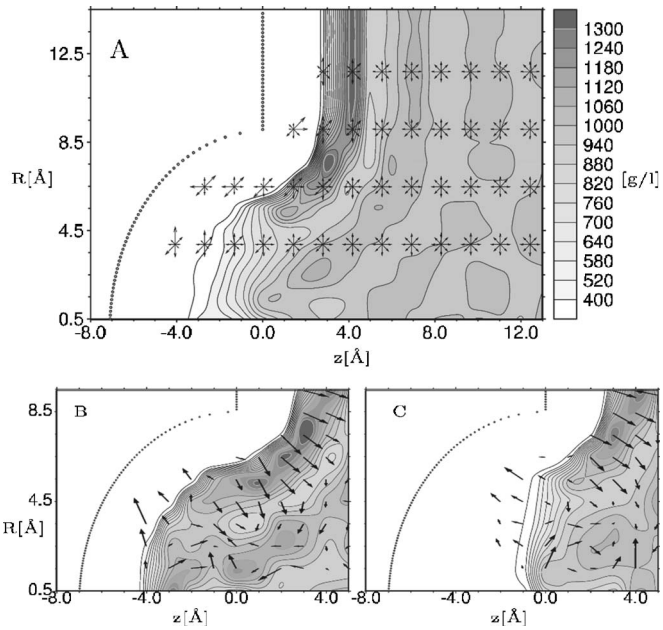

FIG. 4. (A) Average water density and dipole moment orientations divided into eight main directions, projected on the *XZ* plane. [(B) and (C)] Water densities and average dipole moments in "filled" and "empty" states, respectively. Color scale is in g/l. Position of the first layer of hydrophobic wall is marked by dots. Coordinates along the *Z* axis are renumbered in such a way that $Z=0$ corresponds to the first layer of hydrophobic particles in flat regions of wall. These and all other similar plots were prepared with the XFARBE program (Ref. 69).

$$\bar{\tau} = \frac{\tau}{\beta}\Gamma\left(\frac{1}{\beta}\right),$$

where $\Gamma(z)$ is the gamma function.

III. RESULTS AND DISCUSSION

A. Structural properties

Water density and average dipole orientations are presented in Fig. 4. The first, second, as well as the weak third hydration layers are clearly distinguished along flat and convex parts of the wall. The first and second hydration layers are separated by region of decreased density. In general the water density exhibits layering up to 12 Å away from flat surfaces.

Average dipole vector of water molecules occupying the first hydration layer along flat and convex regions is pointed away from the surface. It is worth stressing, however, that the most predominant dipole vector orientation is parallel to the surface[15,16] and is averaged out due to wall anisotropy. This ordering is rather weak and does not extend any further than to the density minimum separating first and second hydration layers.

In concave regions the first solvation layer is no longer present and the average water density smoothly drops off to zero at the bottom of the pocket, forming a density profile similar to that of the water-vapor interface.[41] It should be noted that it is not a static picture: water density inside the pocket undergoes large fluctuations, ranging from almost bulklike value to zero (see Sec. III B). That is why we con-

Downloaded 08 Nov 2006 to 144.74.27.1. Redistribution subject to AIP license or copyright, see http://jcp.aip.org/jcp/copyright.jsp

sider two separate states: a "filled" pocket, when number of water molecules is greater or equal to the average (6), and an "empty" pocket in the opposite case.

In the filled [Fig. 4(b)] state a kind of layering is present, however, layers do not cover concave parts of the wall. They rather extend from the bulk for as long as possible and terminate at the bottom of the pocket. Although a density reduction in proximity to the hydrophobic medium is rather steep, there is no density maximum characteristic for a wet interface. Such state seems to be similar to the contact state observed earlier by Wallqvist *et al.*[41]

In the empty [Fig. 4(c)] state most water molecules concentrate at the entrance to the pocket, leaving deeper parts unoccupied, regardless of favorable interaction potential at the bottom region.

In both states average dipole vectors of water molecules occupying the pocket are less oriented than those along flat portions of the wall and exhibit a tendency to point towards the hydrophobic medium. One should keep in mind, however, that again, the most predominant orientation is parallel to the surface and is not depicted due to averaging.

On average, no layering of water density at concave surface is observed which contrasts with results obtained by Chau.[43] He considered hydrophobic hemispherical cavities constructed from CH united atoms placed at vertices of tessellated icosahedra and solvated with simple point charge extended (SPC/E) water molecules. Simulations were performed in the *NVE* ensemble after preliminary equilibration in the *NPT* ensemble. Since radii of simulated hemispheres were similar to the radius of our pocket, the difference is likely to originate from the strength of attractive interactions between water and hydrophobic surface. Indeed, in his next paper devoted to identical system,[62] Chau admits that hydrophobic "atoms" located in vertices of his tessellated icosahedra are closer to each other than in an alkane molecule, while having unchanged parameters of Lennard-Jones potential. Furthermore, a question arises to what extent electrostatic interactions between water molecules located on both sides of a thin, single layer solute could contribute to effective attraction towards it, making it "less hydrophobic" than expected. Assuming angle averaged dipole-dipole orientation we estimate by using Keesom equation[63] that at a temperature of 300 K, two SPC/E water molecules, being 7 Å apart, interact with attractive potential of magnitude of 0.06 kcal/mol which is about one-half of a typical well depth of Lennard-Jones potential. When summed up with van der Waals interactions with solute atoms as well as with water molecules arranged in a dense solvation layer on the opposite side of the solute, it is likely to result in a much more attractive potential than in our case.

To understand better water structure and behavior we analyzed the average potential energy per single water molecule at a given location. Such potential energy U can be subdivided into a wall-solvent term U_{ws}, defined as the interaction of water molecule with all pseudoatoms constituting the wall, and solvent-solvent term U_{ss}, defined as half of the interaction energy (time averaged) of a water molecule at the given location with other water molecules (being less than 8 Å apart),

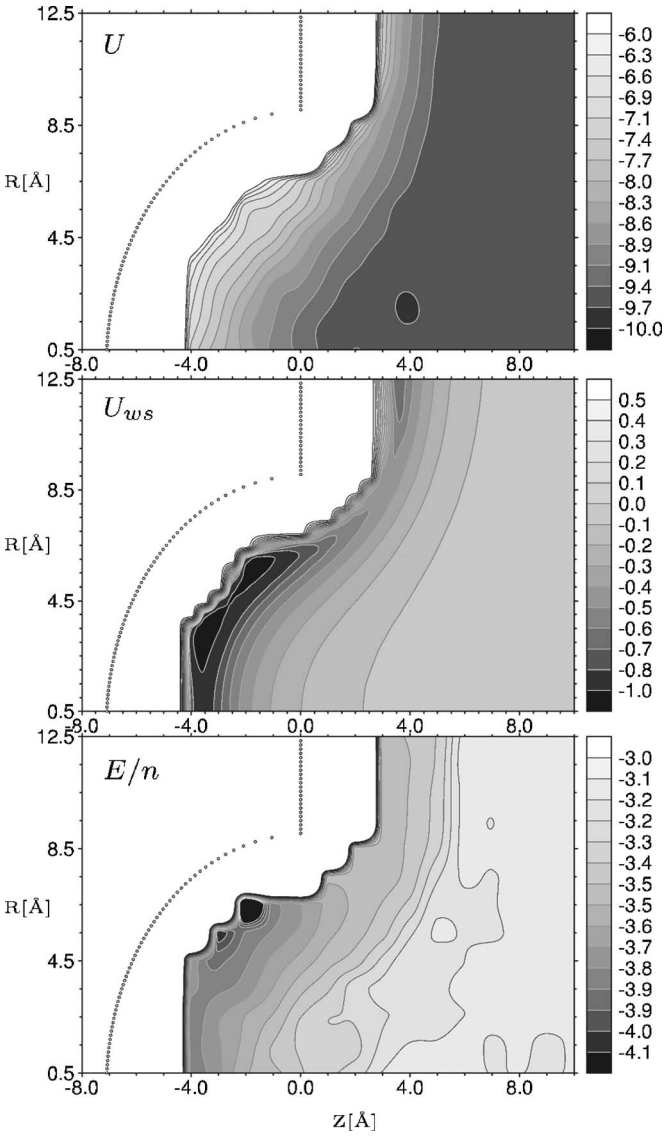

FIG. 5. U—average potential energy (kcal/mol) of a single solvent molecule in the system. U_{ws}—potential energy (in kcal/mol) of interaction between wall and a single solvent molecule. E/n—average energy (kcal/mol) per water-water interaction, including only nearest neighbors, being $\leqslant 4$ Å apart.

$$U = U_{ws} + U_{ss}.$$

As can be seen in Fig. 5, the border of region where repulsive water-wall interaction energy is greater than 0.6 kcal/mol ($\approx 1 k_B T$) extends to about 2.5 Å from the first layer of CH_2 pseudomolecules. The strongest attractive wall-water interactions of magnitude of 1 kcal/mol occur at concave parts of the pockets. In general, inside the whole pocket the interaction potential is attractive and lower than −0.2 kcal/mol.

Within the bulk region a single water molecule contributes about −9.6 kcal/mol to the system energy—a value similar to reported in other studies.[10,64] At the flat water-wall interface the average energy per water molecule rises to about −7.5 kcal/mol. The increase in potential energy with respect to the bulk value is observed in a thin, 2.5 Å layer of solvent, involving only the first hydration shell. In the same region the strengthening of water-water interaction (∼

Downloaded 08 Nov 2006 to 144.74.27.1. Redistribution subject to AIP license or copyright, see http://jcp.aip.org/jcp/copyright.jsp

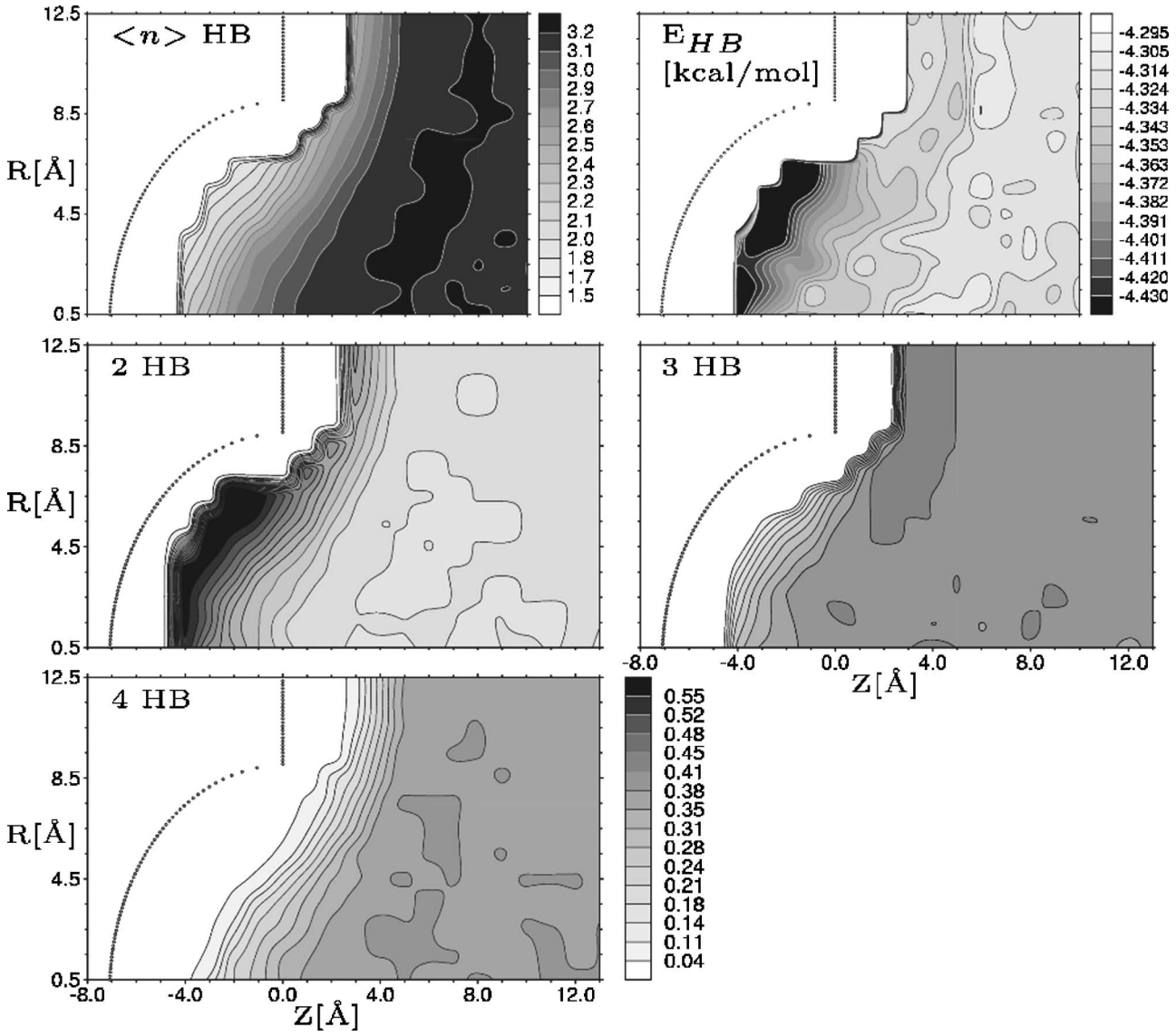

FIG. 6. Hydrogen bonding properties: average number of hydrogen bonds ($\langle n \rangle$HB), average single HB energy (E_{HB}, in kcal/mol), and fractions of water molecules forming particular number (2, 3, and 4) of hydrogen bonds.

−0.5 kcal/mol per water-water pair with respect to value in the bulk) is observed, which partly compensates unfavorable energy change due to loss of nearest neighbors.

As expected, inside the pocket the average energy per water molecule is less favorable than in the bulk, gradually rising up to −6.5 kcal/mol at the bottom (Fig. 5). The decrease in number of neighboring solvent molecules is accompanied by the increase in average quality of remaining interactions. As appears from hydrogen bonding analysis (see below) this increase is caused by the increase of fraction of hydrogen-bonded nearest neighbors rather than by strengthening of particular interaction types.

Hydrogen bonding properties are shown in Fig. 6. In the bulk region, mean hydrogen bond (HB) number per water molecule is 3.19. 40% of water molecules forms three HBs, and 37% and 17% form four and two HBs, respectively. Mean energy of a single HB is −4.32 kcal/mol. These results are in a very good agreement with other studies, involving TIP4P molecules.[56]

In the first hydration layer, close to flat areas of the wall, fraction of water molecules forming three hydrogen bonds is increased. This is in agreement with well documented earlier observations,[16,17] suggesting that in the planar interface water molecules tend to sacrifice one possible hydrogen bonding interaction but then, due to reduced translational and rotational mobility, are able to maintain three other, relatively strong hydrogen bonds. The second hydration shell is formed of water molecules having slight preference for making four hydrogen bonds.

An average HB number decreases inside the pocket: four HB population vanishes in favor of two HB population, which is particularly well represented in concave areas, where geometric constraints imposed on water molecules make forming more than two HBs impossible. Interestingly three HB fraction remains quite intact until almost 2 Å inside the pocket.

In all cases the decrease in number of HB is accompanied by the increase in their quality. A water molecule losing one HB has weaker geometric constraints for making the remaining bonds. On the other hand, the observed difference

Downloaded 08 Nov 2006 to 144.74.27.1. Redistribution subject to AIP license or copyright, see http://jcp.aip.org/jcp/copyright.jsp

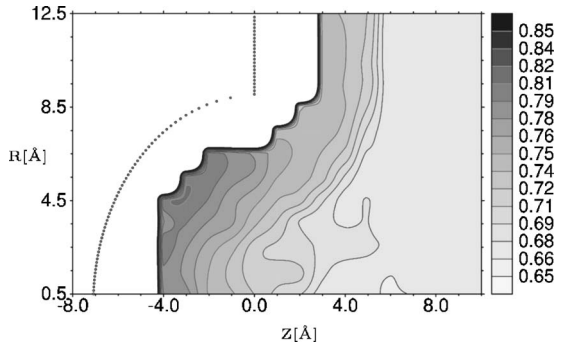

FIG. 7. Fraction of neighboring water molecules, being less than 3.4 Å apart from the central molecule, that forms a hydrogen bond with it.

between energy of the "strongest" HB that is observed at the bottom of the pocket and the "bulk" HB energy is in only of the order of 0.1 kcal/mol, so a tightening of HB cannot be considered as a mechanism of compensation for energy losses due to loss of nearest neighbors.

Instead, we think that changes in fraction of hydrogen-bonded nearest neighbors are important. In the bulk region only about 60% of nearest neighbors (NNs), being less than 3.4 Å apart from the central molecule, form HB with it (Fig. 7)—remaining 40% interacts, relatively poor, giving average energy per NN about −3 kcal/mol (see Fig. 5). These "poor contacts" are first that are lost when water molecule loses its NN: inside the pocket most water molecules form only two HBs, but they account for interactions with more than 80% of NN.

B. Dynamic properties

Time evolution of pocket occupancy is displayed in Fig. 8. As can be observed, the number of water molecules (n_{H_2O}) inside the pocket varies from 0 (empty pocket) up to 18 (liquidlike state) with an average value of 6.4. When compared to bulk water, confined in identical volume, average density is two times smaller and presents significantly larger oscillations. Similar density depression and fluctuations were observed inside cylindrical hydrophobic pores of subnanometer radii.[44]

Free energy profile for water inside the pocket (Fig. 9) reveals differences not greater than $1k_BT$ (0.6 kcal/mol) between states corresponding to $0 \leqslant n_{H_2O} \leqslant 13$. For larger numbers of water molecules a "fluidlike" state is reached and free energy of the system rises in a similar way as in bulk. There is a very weak minimum around $n_{H_2O}=5$, denoting a slight preference for a "vaporlike" state, however, in general, free energy profile for $n_{H_2O} \leqslant 11$ may be considered as flat.

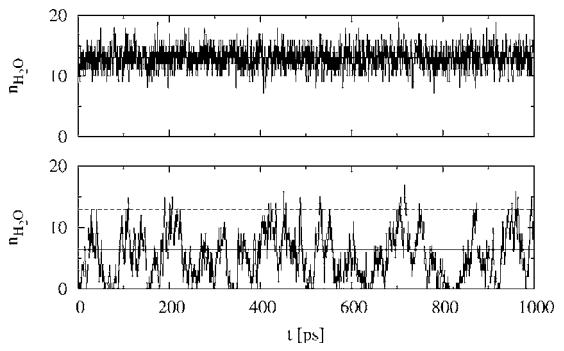

FIG. 8. A number of water molecules (n_{H_2O}) occupying the cavity (lower plot) and a representative bulk volume (upper plot) during a 1 ns simulation. In the lower plot solid line denotes the average cavity occupancy and dashed line denotes the average occupancy observed in the bulk.

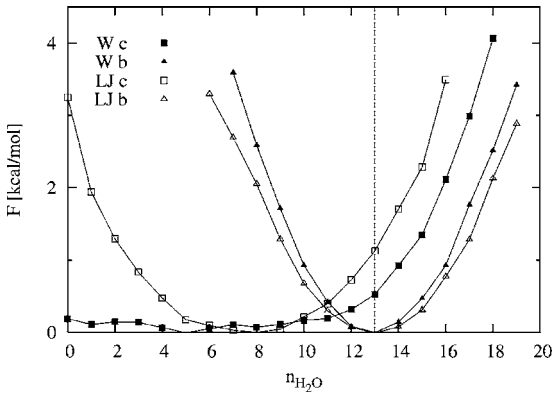

FIG. 9. Free energy profiles (in kcal/mol) for water inside the cavity (Wc), bulk water (Wb), Lennard-Jones fluid inside the cavity (Lc), and bulk LJ fluid (Lb). Energy values were shifted to have zero as a minimum in all cases. Vertical dashed line denotes average number of water molecules (13) confined in considered volume for water density 997 g/l.

From microscopic point of view average chemical potential of water molecule entering the pocket that is filled with less than 11 other molecules is equal to the chemical potential of water molecule in the bulk. Loss of about 2.5 kcal/mol of energy (see Fig. 5) must be compensated by the increase of entropy upon entering the pocket. Such balance seems to exist over surprisingly wide range of pocket occupancies.

According to analytical mean-field model for water in infinite cylindrical hydrophobic micropores presented by Giaya and Thompson,[65] kind of thermodynamically stable phase of confined water depends strongly on attractive component of wall-water interaction potential as well as on pore radius. Although the geometry of our system is not a cylindrical one, a qualitative picture may be similar, suggesting that for a chosen water-wall interaction potential, radius of analyzed pocket may be close to critical one. Indeed, similar simulation carried out with pocket of 5 Å radius (results not shown here) resulted in free energy monotonically rising for $n_{H_2O}>0$. It indicates a clear preference for a vaporlike state of pockets smaller than considered in current study.

Free energy profile for a pocket region is rather different from the one obtained for bulk water. In the latter case a parabolic curve is seen that confirms a Gaussian nature of bulk water density fluctuations.[66,67] As expected, a minimum in free energy is reached for a number of water molecules (13) that corresponds to standard water density in a considered volume. Similar parabolic curve was obtained for Lennard-Jones bulk density fluctuations.

Interestingly free energy profile for LJ particles occupying the pocket is different than the one obtained for water. There is one clear minimum for $n_{LJ}=8$ and any further decrease in occupancy is unfavorable. The difference between free energies corresponding to this minimum and to $n_{LJ}=13$ (bulk density) is higher than in water.

Downloaded 08 Nov 2006 to 144.74.27.1. Redistribution subject to AIP license or copyright, see http://jcp.aip.org/jcp/copyright.jsp

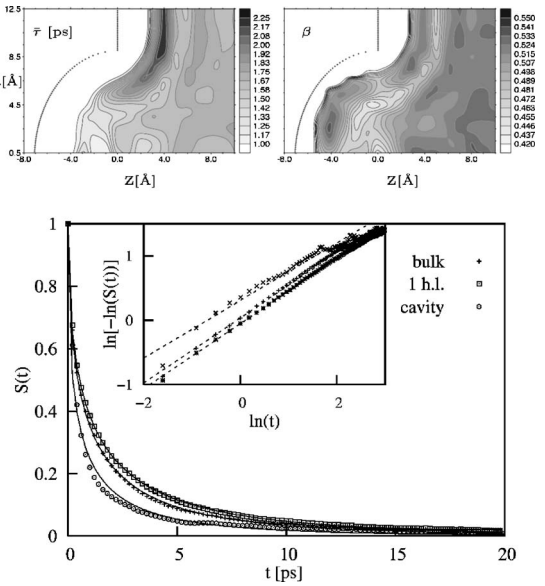

FIG. 10. Average residence time $\bar{\tau}$ and values of β parameter. $S(t)$ plots for three representative cases: bulk water, first hydration layer (1 h.l.), and cavity with fitted KWW curves. Inset shows a log-log plot of the same values.

Possibly these differences result from collective behavior of water molecules. The process of filling and emptying the pocket seems to occur as expansion and retraction of bulklike fluid, happening in tens of picosecond time scale (see Fig. 8), rather than as stochastic movement of individual molecules that would be characteristic for more or less evenly distributed vapor. Reason for this may be strong intermolecular interactions, preventing a single water molecule from going far away from its neighbors. Strong intermolecular interactions, resulting in relatively high surface tension of water, may be also responsible for smaller than in the case of LJ fluid increase in free energy associated with reaching a bulk density inside the pocket: less additional wall-solvent interactions are needed to keep a confined fluid dense.

Dynamic properties, evaluated in terms of average residence time $\bar{\tau}$ and β parameter, are displayed in Fig. 10. $S(t)$ plots are presented on the accompanying graph, along with fitted WWK curves for three representative cases: bulk water, first hydration layer, and center of the pocket.

Time dependence of the survival function seems to be very well approximated by a stretched exponential model, particularly in the case of bulk and first hydration layer regions. Slightly worse fit obtained in the case of pocket region may be the result of more complex water dynamics in this area.

In general all three curves show similar trend of fast initial decay followed by a slower decay, which is consistent with solvent relaxation profiles observed in other studies.[68] A fast component of survival function is usually ascribed to vibrational and librational motions of water molecules within microscopic volumes enclosed by nearest neighbors. Molecules initially located close to the border of a given site may easily cross it forward and backward, contributing to rapid decrease of average population. The remaining slow component reflects a real migration of water molecules from their initial location. Such existence of at least two time scales in relaxation process gives rise to relatively small values of β parameters.

For the bulk water the following values were observed: $\bar{\tau}=1.81$ ps and $\beta=0.503$. In the first hydration layer residence time is longer than in bulk (2.16 ps), with similar β value (0.506). Region of decreased water density, separating the first and the second solvation layers, manifests itself by decreased residence time and β value.

Inside the pocket average residence times are noticeably decreased: $\bar{\tau}\approx 1.16$ ps with respect to bulk water. It is likely to confirm a picture of enhanced mobility of solvent molecules in concave hydrophobic areas.[42] Value of β parameter is also decreased to 0.458 in the center of pocket, giving evidence of broad distribution of residence times. It is a result of complexity of water behavior in this area: there are periods when the pocket is filled with water of bulk density as well as periods when it is virtually empty. Time scale of such fluctuations is larger (see above) than observed residence times. Residence times computed for sites inside the pocket are thus averaged over various regimes of water molecule behavior.

A close inspection of $S(t)$ plot for the pocket region reveals a slight increase in fraction of survived molecules after about 6 ps time. We think that it may result from the fact that once entering the pocket a water molecule, moving relatively freely inside the restricted volume, has a chance to occasionally reenter its initial location.

Interestingly, values of β parameters in the region closest to the concave wall are larger than in the center of the pocket. They are accompanied by residence times shorter than 1 ps and thus invisible in the $\bar{\tau}$ plot. They are likely to represent those areas that are relatively seldom visited by water molecules due to wall repulsion. Once entering such region a water molecule leaves it very fast and resulting distribution of relaxation times is narrower than in the center of the pocket.

In general residence times at a given location seem to correlate with average local water density. It seems to be reasonable since the denser is the solvent the harder is for its molecule to leave their initial locations. Such correlation, however, is not observed in studies of water residence times around proteins.[58] Furthermore it is reported that the longest residence times are observed either in the cavities inside the protein or in the grooves and concave regions.

It is likely to confirm the importance of specific local interactions, mainly hydrogen bonds, at the protein surface for water residence times. In our case, despite of having attractive component in interaction potential, the hydrophobic wall cannot provide any localized interactions. It allows for relatively unrestricted movement of water molecules tangential to its surface, which may affect residence times. Apart from that, it should be noted that in the case of our system, involving relatively deep, entirely hydrophobic pocket, a collective behavior of water molecules leads to intermittent solvation and desolvation of the whole considered volume. Thus it is impossible for a single solvent molecule to stay long at a given location. Recently similar results have been demonstrated[40] in all atom, explicit solvent simulation of

Downloaded 08 Nov 2006 to 144.74.27.1. Redistribution subject to AIP license or copyright, see http://jcp.aip.org/jcp/copyright.jsp

mouse major urinary protein (MUP) that has a deep, hydrophobic binding pocket. Furthermore authors confirmed experimentally that desolvation of the binding site has a little contribution to ligand binding free energy, which remains in agreement with our free energy curves.

IV. CONCLUSIONS

In this work we have studied the structural and dynamic properties of water in proximity of a hemispherical hydrophobic pocket of 8 Å radius embedded in a hydrophobic wall. We have observed a drying phenomenon inside the pocket, manifested as significant depression of water average density and shortening of solvent residence times. Such drying was not present at flat portions of wall even though attractive interactions in those areas were weaker than inside the pocket. It seems to indicate that not only the strength of attractive interactions but also the topography of the surface influences character of hydrophobic hydration.

We have found that substantial fluctuations of pocket occupancy, having a time scale of tens of picoseconds, occur as expansion and retraction of a bulklike fluid rather than as individual movement of solvent molecules that would be characteristic for a "vaporlike" state. It indicates a collective behavior of water molecules.

Free energy differences accompanying changes in pocket occupancy from empty to filled state are smaller than $1k_BT$, suggesting that, for applied wall-water interaction potential, the considered pocket radius is close to the critical one for transition from a thermodynamically stable vapor phase to a liquid phase.

Our system may be considered as a rather idealized model of hydrophobic binding pocket. Nevertheless obtained results indicate that contribution to hypothetic binding free energy, resulting from desolvation of such a binding site, may be not predicted correctly with the use of surface area based models. Furthermore a water behavior inside the pocket seems to be governed by its architecture as a whole and not only by local surface curvature and hydrophobicity.

Next step of our investigation will be devoted to the analysis of interaction of hydrophobic pockets with model particles.

ACKNOWLEDGMENTS

This study was supported by the European Centre of Excellence "MAMBA" (Project No. QLAM-2001-00383), the National Centre of Excellence, "BioExploratorium," and funds of BST 1059/BF and BW-1684/BF. Computations were carried out in the Interdisciplinary Centre of Mathematical and Computational Modeling at Warsaw University.

[1] N. T. Southall, K. A. Dill, and A. D. J. Haymet, J. Phys. Chem. B **106**, 521 (2002).
[2] W. Blokzijl and J. B. F. N. Engberts, Angew. Chem., Int. Ed. Engl. **32**, 1545 (1993).
[3] C. Tanford, *The Hydrophobic Effect: Formation of Micelles and Biological Membranes* (Wiley, New York, 1973).
[4] P. L. Privalov and G. I. Makhatadze, J. Mol. Biol. **232**, 660 (1993).
[5] L. Y. Zhang, E. Gallicchio, R. A. Friesner, and R. M. Levy, J. Comput. Chem. **22**, 597 (2001).
[6] V. V. Yaminsky and E. A. Vogler, Curr. Opin. Colloid Interface Sci. **6**, 342 (2001).
[7] L. R. Pratt, Annu. Rev. Phys. Chem. **53**, 409 (2002).
[8] J. H. Griffith and H. A. Sheraga, J. Mol. Struct. **682**, 97 (2004).
[9] P. Wernet, D. Nordlund, U. Bergmann *et al.*, Science **304**, 995 (2004).
[10] S. R. Durell and A. Wallqvist, Biophys. J. **71**, 1695 (1996).
[11] C. Czaplewski, A. Liwo, D. R. Ripoll, and H. A. Scheraga, J. Phys. Chem. B **109**, 8108 (2005).
[12] R. M. Lynden-Bell and J. C. Rasaiah, J. Chem. Phys. **107**, 1981 (1997).
[13] N. Matubayasi, L. H. Reed, and R. M. Levy, J. Phys. Chem. **98**, 10640 (1994).
[14] N. Matubayasi and R. M. Levy, J. Phys. Chem. **100**, 2681 (1996).
[15] L. R. Pratt and A. Pohorille, Chem. Rev. (Washington, D.C.) **102**, 2671 (2002).
[16] C. Y. Lee and J. A. McCammon, J. Chem. Phys. **80**, 4448 (1984).
[17] S. H. Lee and P. J. Rossky, J. Chem. Phys. **100**, 3334 (1993).
[18] K. Lum, D. Chandler, and J. D. Weeks, J. Phys. Chem. B **103**, 4570 (1999).
[19] D. M. Huang and D. Chandler, Proc. Natl. Acad. Sci. U.S.A. **97**, 8324 (2000).
[20] D. M. Huang and D. Chandler, J. Phys. Chem. B **106**, 2047 (2002).
[21] D. M. Huang, P. L. Geissler, and D. Chandler, J. Phys. Chem. B **105**, 6704 (2001).
[22] P. R. ten Wolde, S. X. Sun, and D. Chandler, Phys. Rev. E **65**, 011201 (2001).
[23] F. H. Stillinger, J. Solution Chem. **2**, 141 (1973).
[24] H. S. Ashbaugh and L. R. Pratt, Rev. Mod. Phys. **78**, 156 (2006).
[25] D. A. Doshi, E. B. Watkins, J. N. Israelachvili, and J. Majewski, Proc. Natl. Acad. Sci. U.S.A. **102**, 9458 (2005).
[26] D. Schwendel, T. Hayashi, R. Dahint, A. Pertsin, M. Grunze, R. Steitz, and F. Schreiber, Langmuir **19**, 2284 (2003).
[27] T. R. Jensen, M. Ø. Jensen, N. Reitzel, K. Balashev, G. H. Peters, K. Kjaer, and T. Bjørnholm, Phys. Rev. Lett. **90**, 086101 (2003).
[28] X. H. Zhang, N. Maeda, and V. S. J. Craig, Langmuir **22**, 5025 (2006).
[29] R. Steitz, T. Gutberlet, T. Hauss, B. Klosgen, R. Krastev, S. Schemmel, A. C. Simonsen, and G. H. Findenegg, Langmuir **19**, 2409 (2003).
[30] J. W. G. Tyrrell and P. Attard, Phys. Rev. Lett. **87**, 176104 (2001).
[31] O. I. Vinogradova, N. F. Bunkin, N. V. Churaev, O. A. Kiseleva, A. V. Lobeyev, and B. W. Ninham, J. Colloid Interface Sci. **173**, 443 (1995).
[32] A. Carambassis, L. C. Jonke, P. Attard, and M. W. Rutland, Phys. Rev. Lett. **80**, 5357 (1998).
[33] Y. Takata, J.-H. J. Cho, B. M. Law, and M. Aratono, Langmuir **22**, 1715 (2006).
[34] E. E. Meyer, Q. Lin, and J. N. Israelachvili, Langmuir **21**, 256 (2005).
[35] X. Huang, C. J. Margulis, and B. J. Berne, Proc. Natl. Acad. Sci. U.S.A. **100**, 11953 (2003).
[36] D. Bratko, R. A. Curtis, H. W. Blanch, and J. M. Prausnitz, J. Chem. Phys. **115**, 3873 (2001).
[37] N. Choudhury and B. M. Pettitt, J. Phys. Chem. B **109**, 6422 (2005).
[38] N. Choudhury and B. M. Pettitt, J. Am. Chem. Soc. **127**, 3556 (2005).
[39] Y.-K. Cheng and P. J. Rossky, Nature (London) **392**, 696 (1998).
[40] E. Barratt, R. J. Bingham, D. J. Warner, C. A. Laughton, S. E. V.Phillips, and S. W. Homans, J. Am. Chem. Soc. **127**, 11827 (2005).
[41] A. Wallqvist, E. Gallicchio, and R. M. Levy, J. Phys. Chem. B **105**, 6745 (2001).
[42] J. Faeder and B. M. Ladanyi, J. Phys. Chem. B **104**, 1033 (2000).
[43] P.-L. Chau, Mol. Phys. **99**, 1289 (2001).
[44] O. Beckstein and M. S. P. Sansom, Proc. Natl. Acad. Sci. U.S.A. **100**, 7063 (2003).
[45] G. Hummer, J. C. Rasaiah, and J. P. Noworyta, Nature (London) **414**, 188 (2001).
[46] W. L. Jorgensen, J. Chandrasekhar, J. D. Madura, R. W. Impey, and M. L. Klein, J. Chem. Phys. **79**, 926 (1983).
[47] L. R. Pratt and A. Pohorille, Proc. Natl. Acad. Sci. U.S.A. **89**, 2995 (1992).
[48] M. P. Allen and D. J. Tildesley, *Computer Simulation of Liquids* (Oxford University Press, New York, 1987).
[49] H. C. Andersen, J. Chem. Phys. **72**, 2384 (1980).
[50] S. E. Feller, Y. Z. Richard, W. Pastor, and B. R. Brooks, J. Chem. Phys. **103**, 4613 (1995).
[51] B. R. Brooks, R. E. Bruccoleri, B. D. Olafson, D. J. States, S. Swaminathan, M. Karplus, J. Comput. Chem. **4**, 187 (1983).
[52] S. Nose, J. Chem. Phys. **81**, 511 (1984).
[53] W. G. Hoover, Phys. Rev. A **31**, 1695 (1985).

Downloaded 08 Nov 2006 to 144.74.27.1. Redistribution subject to AIP license or copyright, see http://jcp.aip.org/jcp/copyright.jsp

[54] J.-P. Ryckaert, G. Ciccotti, and H. J. C. Berendsen, J. Comput. Phys. **23**, 327 (1977).
[55] S. E. Feller, R. W. Pastor, A. Rojnuckarin, S. Bogusz, and B. R. Brooks, J. Phys. Chem. **100**, 17011 (1996).
[56] A. G. Kalinichev and J. D. Bass, J. Phys. Chem. A **101**, 9720 (1997).
[57] R. W. Impey, P. A. Madden, and I. R. McDonald, J. Phys. Chem. **87**, 5071 (1983).
[58] V. A. Makarov, B. K. Andrews, P. E. Smith, and B. M. Pettitt, Biophys. J. **79**, 2966 (2000).
[59] R. Abseher, H. Shreiber, and O. Steinhauser, Proteins: Struct., Funct., Genet. **25**, 366 (1996).
[60] S. Yoshioka, Y. Aso, and S. Kojima, Pharm. Res. **18**, 256 (2001).
[61] C. P. Lindsey and G. D. Patterson, J. Chem. Phys. **73**, 3348 (1980).
[62] P.-L. Chau, Mol. Phys. **101**, 3121 (2003).
[63] J. Israelachvilli, *Intermolecular and Surface Forces* (Academic, New York, 1992).
[64] E. Gallicchio, M. M. Kubo, and R. M. Levy, J. Phys. Chem. B **104**, 6271 (2000).
[65] A. Giaya and R. W. Thompson, J. Chem. Phys. **117**, 3464 (2002).
[66] G. Hummer, S. Garde, A. E. Garcia, A. Pohorille, and L. R. Pratt, Proc. Natl. Acad. Sci. U.S.A. **93**, 8951 (1996).
[67] D. Chandler, Phys. Rev. E **48**, 2898 (1993).
[68] C. Rocchi, A. R. Bizzarri, and S. Cannistraro, Phys. Rev. E **57**, 3315 (1998).
[69] A. Preusser, ACM Trans. Math. Softw. **15**, 79 (1998).

Downloaded 08 Nov 2006 to 144.74.27.1. Redistribution subject to AIP license or copyright, see http://jcp.aip.org/jcp/copyright.jsp